Carbohydrate Polymers 286 (2022) 119298

Contents lists available at ScienceDirect

Carbohydrate Polymers

journal homepage: www.elsevier.com/locate/carbpol

# Insights into pectin dominated enhancements for elimination of toxic Cd and dye coupled with ethanol production in desirable lignocelluloses

Hua Yu [a,b], Meng Hu [a], Zhen Hu [a,b], Fei Liu [a,b], Haizhong Yu [b], Qiaomei Yang [a,b], Hairong Gao [a,b], Chengbao Xu [a,b], Meiling Wang [a], Guifen Zhang [a], Yun Wang [c], Tao Xia [a,b], Liangcai Peng [a,b], Yanting Wang [a,b,*]

[a] Biomass & Bioenergy Research Center, College of Plant Science & Technology, Huazhong Agricultural University, Wuhan 430070, China
[b] Laboratory of Biomass Engineering & Nanomaterial Application in Automobiles, College of Food Science & Chemical Engineering, Hubei University of Arts & Science, Xiangyang, China
[c] College of Science, Huazhong Agricultural University, Wuhan 430070, China

ARTICLE INFO

*Keywords:*
Plant cell wall
Uronic acids
Biosorbents
Biomass saccharification
Phytoremediation

ABSTRACT

Pectin is a minor wall polysaccharide with potential applications for bioproducts. Despite the application of specific plants and biomass-based sorbents for environmental remediation, little has been reported about characteristic roles of pectin. Using the natural rice mutant (*Osfc16*) treated with Cd, this study explored that pectin could predominately enhance Cd accumulation with lignocellulose, mainly due to remarkably raised uronic acids deposition. The Cd-treatment further reduced lignocellulose recalcitrance for significantly enhanced biomass saccharification and bioethanol production along with almost complete Cd release. Using all remaining fermentation rice residues that are of typical ribbon-structure and large surface, this study generated novel biosorbents by optimal chemical oxidation with the pectin extraction from citrus peels, and examined consistently raised Cd and methylene blue (MB) adsorption capacities. Therefore, this work has proposed a mechanism model about multiple pectin enrichment roles for Cd and MB removals in agricultural and industry locations with full lignocellulose utilization towards bioethanol production.

## 1. Introduction

Lignocellulose is mainly composed of three wall polymers (cellulose, hemicellulose, lignin), which not only determines biomass recalcitrant property, but is also involved in trace metal remediation (Wang et al., 2021). As a minor wall polymer, pectin also plays an important role in plant growth and development with potential utilization for valuable bioproduction (Jensen et al., 2018; Liang et al., 2020; Wang et al., 2015; Xu et al., 2021). However, much remains unknown about pectin characteristics for biomass saccharification and trace metal phytoremediation. Citrus is an important fruit tree grown in non-agricultural lands, but it also produces large amounts of peel residues wastes that are released into the environment (Perazzini, Perazzini, Freire, Freire, & Freire, 2021).

Phytoremediation has been broadly applied for trace metal elimination in contaminated locations (Cheng et al., 2018; Cheng et al., 2019). In general, growing desirable crops is increasingly considered as a green and economical bioremediation technology for the agricultural soil contained with small amounts of trace metals (Hossain, Bhattacharyya, & Aditya, 2014; Qu et al., 2018). In particular, cadmium (Cd) has been examined as a major trace metal contaminated in agricultural lands around the world (Dmuchowski, Gozdowski, & Baczewska, 2011; Ramrakhiani et al., 2017; Wu et al., 2020) and various phytoremediation technologies like phytoextraction and phytoaccumulation (Cheng et al., 2018; Wu et al., 2020), and adsorption technologies have been implemented (López-Maldonado, Oropeza-Guzman, Jurado-Baizaval, & Ochoa-Terán, 2014; García, Oropeza-Guzmán, Argüelles Monal, & López-Maldonado, 2019; López-Maldonado & Oropeza-Guzmán, 2021). However, although special crop species could accumulate Cd with lignocellulose residues, much is unknown about how

*Abbreviations:* Cd, cadmium; MB, methylene blue; NaOH, sodium hydroxide; FR, fermentation residues; CP, citrus peel.

* Correspondent author at: Biomass & Bioenergy Research Center, College of Plant Science & Technology, Huazhong Agricultural University, Wuhan 430070, China.
*E-mail address:* wyt@mail.hzau.edu.cn (Y. Wang).
*URL:* http://bbrc.hzau.edu.cn (Y. Wang).

https://doi.org/10.1016/j.carbpol.2022.119298
Received 18 November 2021; Received in revised form 23 February 2022; Accepted 24 February 2022
Available online 2 March 2022

lignocellulose is effective to adsorb Cd for remediation. Accordingly, it is important to explore integrated technology, which is not only applicable for efficient Cd removal and recycling, but also for full utilization of lignocellulose without any waste release into the environment.

Chemical dyes are commonly released from textile, leather, paper and plastics industries, and methylene blue (MB) is particularly used for cotton, wood and silk processes (Chen, Zhao, Xie, Liang, & Zong, 2021; Jiang, Wen, Zhu, Liu, & Shao, 2021; Rafatullah, Sulaiman, Hashim, & Ahmad, 2010). As MB could cause serious damage to human health, several physical, chemical and biological methods have been conducted for MB removal (Chen et al., 2017; Safardoust-Hojaghan & Salavati-Niasari, 2017). More recently, non-conventional adsorbents have been implemented for effective adsorption of MB such as natural materials (Halysh et al., 2020), biosorbents (Murray & Örmeci, 2018) and chemical materials (Toledo, Bernardinelli, Sabadini, & Petri, 2020; Wahlström, Steinhagen, Toth, Pavia, & Edlund, 2020), but low-cost and high-efficient biosorbent is increasingly considered for MB elimination from industry liquid wastes.

Crop straws consist of substantial lignocellulose residues convertible for biofuels and biochemicals (Huang et al., 2017). Although cellulosic bioethanol has been evaluated as the excellent additive into petrol fuels for reduced net carbon emission, the natural recalcitrance of lignocellulose leads to a costly biomass conversion with potential secondary waste liberation, which is unacceptable for large-scale bioethanol production (Gao et al., 2021; Li et al., 2018). Hence, genetic modification of plant cell walls has been attempted to reduce lignocellulose recalcitrance in major bioenergy crops, which could cause a cost-effective bioethanol conversion including mild biomass pretreatment, complete enzymatic hydrolysis and durable yeast fermentation (Wang et al., 2016). For instance, selection of genetic mutants and transgenic crop lines has significantly improved lignocellulose features for complete enzymatic saccharification under mild physical and chemical pretreatments performed (Zhang et al., 2011; Wu et al., 2021).

Rice is one of major food crops over the world with large amount of lignocellulose-rich straw (Baramee et al., 2020). In this study, we initially used our previously-selected rice mutant (*Osfc16*) to respectively grow in the water and soil culture pots supplied with high concentrations of Cd, and then examined much raised Cd accumulation in young seedlings and mature straw of the mutant, compared to the wild type (NPB, a classic cultivar). Consequently, this study detected remarkably increased pectin deposition with relatively reduced cellulose level in the mutant, leading to much enhanced biomass enzymatic saccharification for bioethanol fermentation and Cd release for recycling. Furthermore, this work combined the rice mutant residue of yeast fermentation with the rich pectin extracted from citrus peels to generate active biosorbents using oxidation chemicals. Notably, we characterized that the biosorbents were of significantly enhanced Cd and MB adsorptions, and thus proposed an eco-friendly and cost-effective strategy for remediation of trace metals in agricultural soil trace metal remediation and industrial dye removal without any biomass residues liberation.

## 2. Materials and methods

### 2.1. Collection of biomass samples

The general procedure of major experiments performed in this study is described in Fig. S1. The rice (*Oryza sativa* L.) mutant (*Osfc16*) as previously identified (Li et al., 2017) and its wild type/WT, a classic rice cultivar (Nipponbare/NPB), were grown in the soil pots (25.0 kg soil) co-supplied with $CdCl_2$ (CAS No.10108-64-2) at 100 mg/kg dry soil. Prior to the growing of rice seedlings, the soil pots were soaked with water for a few days until the $CdCl_2$ was well mixed with the soil. Each $CdCl_2$ treatment used three soil pots as independent duplication, and each pot contained four rice seedlings. The mature rice straws were collected, dried at 50 °C until constant weight and ground through a 40 mesh screen. The well-mixed powders were stored in a sealed dry container until use. The citrus fruits (Sichuan red orange peel) were purchased from commercial market and citrus peel residues were obtained to extract pectin fraction as described below.

### 2.2. Cd assay in rice residues

The dry biomass sample (0.100 g) was added into the porcelain crucible and transferred to the muffle furnace. The temperature was gradually raised to 200 °C for 1 h, and set at 600 °C for 6–8 h. The ash was dissolved with 1.0% $HNO_3$ (v/v), washed with 1.0% $HNO_3$ for 3 times, and all solutions were collected into a 25 mL volumetric flask. An atomic absorption spectrometer (Agilent 240Z GFAA) was applied for the measurement of Cd content as previously described (Cheng et al., 2019). All samples were measured in independent triplicate.

### 2.3. Wall polymer extraction and determination

A procedure of plant cell wall fractionation was implemented to extract soluble sugars, pectin, hemicellulose and cellulose fractions as previously described by Peng, Hocart, Redmond, and Williamson (2000) and Xu et al. (2012). UV–VIS spectrometer (V-1100D, Shanghai MAPADA Instruments Co.) was used for hexose, pentose and uronic acids assays as previously described by Huang et al. (2017) and Liu et al. (2021). For cellulose assay, the sample was dissolved in 67% $H_2SO_4$ and hexoses were calculated by the anthrone/$H_2SO_4$ method. Hemicelluloses were calculated by determining total hexoses and pentoses of the hemicellulose fraction, and pectin was measured by calculating total hexoses, pentoses and uronic acids of the fraction. In addition, a two-step acid hydrolysis method was applied for total lignin assay according to the Laboratory Analytical Procedure of the National Renewable Energy Laboratory. All experimental analyses were completed in triplicate.

The monosaccharide compositions of hemicelluloses was determined by GC–MS (SHIMADZU GCMS-QP2010 Plus) as previously described by Xu et al. (2012). Trifluoroacetic acid (TFA) and *myo*-inositol were obtained from Aladdin Reagent Inc. *1*-Methylimidazole was purchased from Sigma-Aldrich Co. LLC. Acetic anhydride and acetic acid were obtained from Sinopharm Chemical Reagent Co., Ltd.

### 2.4. Measurement of cellulose features (CrI, DP)

Cellulose crystalline index (CrI) of cellulose samples was measured by Rigaku-D/MAX instrument (Ultima III, Japan) according to the equation: $CrI = 100 \times (I_{200} - I_{am}) / I_{200}$. $I_{200}$ is intensity of the 200 peak ($I_{200}$, $\theta = 22.5°$), which represents crystalline cellulose, whereas $I_{am}$ ($I_{am}$, $\theta = 18.5°$) is the intensity at the minimum between the 200 and 110 peaks, being correspondent to amorphous cellulose. The degree of polymerization (DP) of cellulose samples was determined by the viscosity method subjective to the equation: $DP_{0.905} = 0.75\ [\eta]$ as described previously (Li et al., 2018; Madadi et al., 2022). All the experiments were performed independently in triplicate at 25 ± 0.5 °C.

### 2.5. Characterization of biosorbents

The chemical-crosslinked biosorbents were respectively characterized using our previously-established methods (Xu et al., 2021) including Brunauer–Emmett–Teller (BET) surface area, scanning electron microscopy (SEM), energy dispersive X-ray, X-ray photoelectron spectroscopy(XPS), Fourier transform infrared (FTIR) spectroscopy.

### 2.6. Biomass pretreatment and enzymatic hydrolysis

Alkali pretreatments were performed by adding various concentrations of NaOH (0, 0.5%, 1%, w/v) at 50 °C and 150 rpm for 2 h as previously described (Li, Zhang, et al., 2014; Jin et al., 2016). After

centrifugation at 3000*g* for 5 min, the pellets were washed with 10 mL distilled water for 5 times until pH 7.0. For enzymatic hydrolysis, the pretreated biomass residues were incubated with the final concentration of 1.6 g/L mixed-cellulases (10.6 FPU/g biomass) and xylanase (6.72 U/g biomass) purchased from Imperial Jade Biotechnology Co., Ltd., while co-supplied with 1% Tween-80 as described (Jin et al., 2016). All the experiments were conducted independently in triplicate.

### 2.7. Yeast fermentation and bioethanol measurement

*Saccharomyces cerevisiae* strain (Angel yeast Co., Ltd., Yichang, China) was incubated with total hexoses released from enzymatic hydrolysis of alkali pretreated rice straw for ethanol fermentation as previously described by Jin et al. (2016). The ethanol yield was estimated by $K_2Cr_2O_7$ method as described by Li et al. (2018) and He et al. (2022). Absolute ethanol (99.9%) was used as the standard and the fermentation experiments were conducted independently in triplicate.

### 2.8. Pectin extraction and crosslinking reaction

The well-dried citrus peels powder (1.5 g) was consequentially incubated with 80% ethanol for 2 h, anhydrous ethanol for 12 h and acetone for 10 min to obtain alcohol insoluble residues under air as described by (Pattathil, Avci, Miller, & Hahn, 2012) and. The residues were then incubated with 50 mM ammonium oxalate solution under 150 rpm shaken at 25 °C for 24 h. After centrifugation at 3000*g* for 5 min, the supernatants were collected and added with 1 M NaOH to adjust pH = 9. After dialysis with 3500 kDa bags for 2 days, the sample was collected as pectin extract.

The remaining solid residues from ethanol fermentation were washed with distilled water for three times and dried at 50 °C in an air oven. The well-mixed residues (0.06 g) were added with different dosages (1, 3, 6, 9, 12 mL) of the pectin extract described above, and then incubated with different concentrations of $H_2O_2$ chemicals (0.25%, 0.75%, 1.5%). After mixing well, the residues were shaken under 150 rpm for 3 h at different temperatures (25 °C, 35 °C, 55 °C) and stored as synthesized biosorbents for the following adsorption analysis. All experiments were performed independently in triplicate.

### 2.9. Cd and MB adsorption analysis

The remaining solid residues from ethanol fermentation were washed with distilled water three times, followed with ultra-pure water for another three times. The washed residues were collected, dried at 50 °C in an air oven, and stored as biosorbents samples for the following experiments.

Solutions of $Cd^{2+}$ was prepared by adding $Cd(NO_3)_2 \cdot 4H_2O$ into ultra-pure water at room temperature. Batch adsorption experiments with different types of biosorbents were performed for 4.0 h in 50 mL tubes under 150 rpm shaken. After mixing well, the samples were filtered through a 0.45 μm membrane filter, and the residual $Cd^{2+}$ concentration in the filtrate was detected by flame atomic adsorption spectrophotometer (FAAS HITACHI Z-2000, Japan) equipped with air–acetylene flame as previously described (Xu et al., 2021).

Solution of MB was prepared by adding $C_{16}H_{18}ClN_3S$ into ultra-pure water at room temperature (25 ± 2 °C). Batch adsorption experiments with different types of biosorbents were performed for 4.0 h in 50 mL tubes under 150 rpm shaken. After stirring, the samples were filtered through a 0.45 μm membrane filter, and the residual MB concentration in the filtrate was determined by UV–VIS spectrometer (V-1100D, Shanghai MAPADA Instruments Co.) at $\lambda_{max}$ = 668 nm as described by Hameed and Ahmad (2009).

The amount of adsorption at equilibrium $q_e$ (mg/g) and the adsorption rate (%) were calculated as previously described (Gurgel, Freitas, & Gil, 2008; Xu et al., 2021). Langmuir isotherm and Freundlich isotherm models were characterized as described (Xie et al., 2015) The linear form of the pseudo-second-order equation was plotted as described (Saman et al., 2018). All the assays were conducted independently in triplicate.

### 2.10. Rice seedling hydroponic culture and immunolabeling for wall polysaccharide detection

Rice seeds (WT, *Osfc16*) were soaked in distilled water for 3 days and the germinated rice seeds were put into 96 well plates with water to grow for 15 days. Then, the young seedlings were added with 0.6 mM (141.2 mg/kg water) $CdCl_2$ (CAS No. 10108-64-2) for another 15 days growth, while co-supplied with/without the synthesized biosorbents described above. Meanwhile, the young seedlings were only cultured with distill water as experimental control. Each treatment contained 96 rice seedlings with three biological duplications.

Rice sections (3 mm–5 mm) were cut from leaf vein of rice seedlings, 5 μm thick transverse sections embedded in paraplast plus for immunolabeling. Paraffin sections were de-waxed with xylene and rehydrated through an ethanol series from 100% to 0%. Sections were then washed extensively in PBS, incubated with 5-fold dilution of cell wall glycan-directed monoclonal antibodies (mAbs) followed by 200-fold and 100-fold dilution of anti-mouse IgG linked to fluorescein isothiocyanate (FITC). One glycan-directed mAb was used in this study. CCRC-M38 recognizes epitopes in de-esterified homogalacturonan (pectin). Samples were washed at least three times as described (Yang et al., 2020). FITC fluorescence was observed with an Olympus BX61 microscope equipped with epifluorescence optics as previously described (Yang et al., 2020).

### 2.11. Statistical analysis

Analyses of variance (ANOVA), regression coefficients and Spearman's rank correlation coefficient were respectively accomplished using Superior Performance Software System (SPSS version 16.0, Inc., Chicago, IL). Pair-wise comparisons were conducted between two measurements by Student's *t*-test. The line graph, histogram, and regression analysis for the best fit curve were plotted using Origin 8.5 software (Microcal Software, Northampton, MA). The average values were calculated from the original independent triplicate measurements for these analyses.

## 3. Results and discussion

### 3.1. Remarkably raised Cd accumulation in desirable Osfc16 mutant

Using our previously-identified natural rice mutant (*Osfc16*) defective at cellulose biosynthesis (Li et al., 2017), this study initially detected its Cd accumulation capacity (Fig. 1). While young seedlings were grown with the hydroponic culture supplied with 0.6 mM (141.2 mg/kg water) $CdCl_2$ for 15 days, the *Osfc16* mutant showed much more Cd accumulation than that of the WT (NPB) by over 3-folds (Fig. 1A & B). Meanwhile, this work examined Cd accumulation with rice straws using the soil pots for rice growth supplied with high concentration of $Cd^{2+}$ (100 mg $CdCl_2$/kg dry soil). As a result, the *Osfc16* mutant respectively contained Cd levels at 4.65 μg/g and 14.38 μg/g dry matter in mature stem and leaf tissues, which were significantly higher than those of the WT by 32% and 58% at $p < 0.01$ level (Fig. 1C & D). However, even though grown soil pots supplied with high concentration of Cd, the *Osfc16* mutant accumulated relatively low Cd level at grain tissue, being almost less 9-fold than its leaf tissue (Fig. S2). Hence, the *Osfc16* mutant could consistently accumulate much Cd in almost all lignocellulose residues, and it should be considered as the desirable crop for Cd phytoremediation.

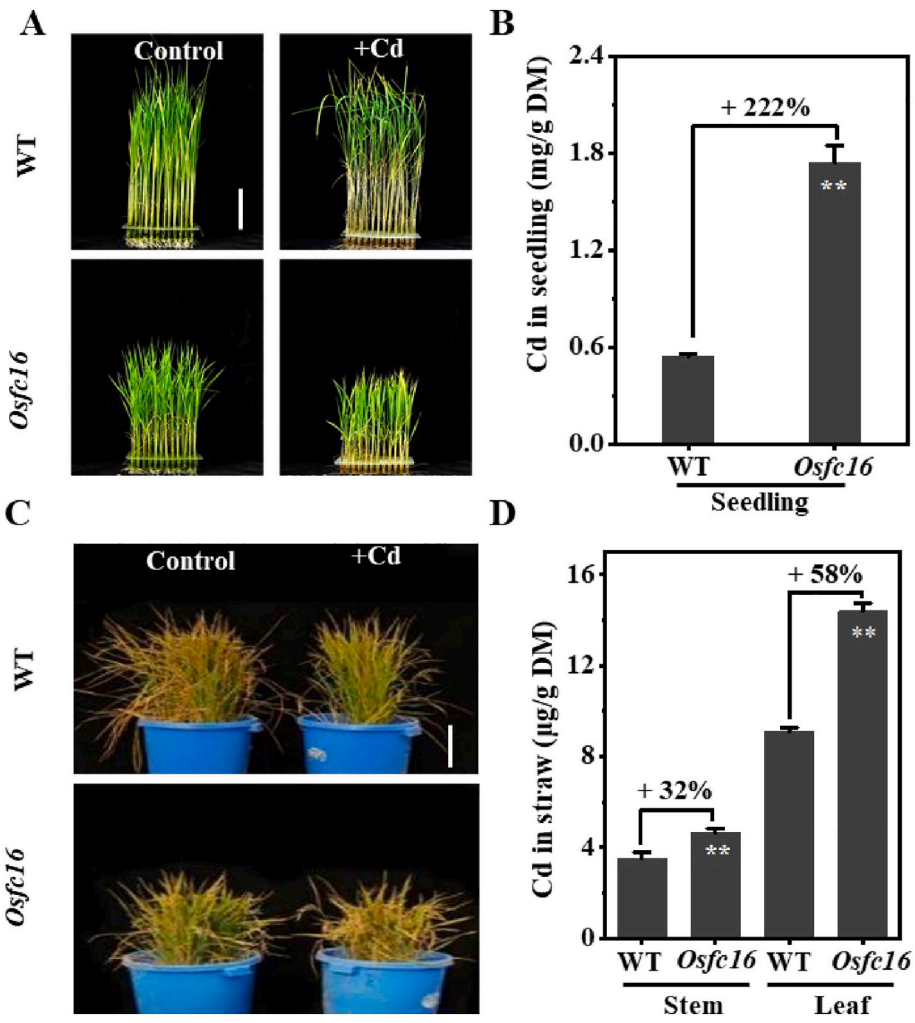


**Fig. 1.** Cd accumulation with lignocellulose tissues of rice mutant (*Osfc16*) and WT (NPB). (A) Images of rice seedlings (scale bar = 5 cm) grown with water culture supplied with 0.6 mM (141.2 mg/kg water) $CdCl_2$ (+Cd) and control (without $CdCl_2$); (B) Cd contents in rice seedling; (C) Images of mature rice straw grown in the soil pots supplied with 100 mg/kg (+Cd) and control (without $CdCl_2$); (D) Cd contents in rice straw (scale bar = 20 cm). * and ** indicated significant difference between two samples by *t*-test at $p < 0.05$ and 0.01 (n = 3). Increased percesntage calculated by subtraction between two samples divided by the control. Bar as mean ± SD (n = 2). DM: dry matter.

### 3.2. Predominately enhanced pectin deposition for large Cd accumulation

As the *Osfc16* mutant could largely accumulate Cd in lignocellulose-rich tissues, this study determined lignocellulose composition in young rice seedlings and mature straws (Table 1). After treatment with Cd, both *Osfc16* mutant and WT showed remarkably raised pectin depositions by 17%–42% with relatively increased hemicellulose levels by 2%–12% in the seeding, stem and leaf tissues examined. Accordingly, significantly reduced cellulose levels by 8%–33% were detected in those tissues, but the lignin contents were altered marginally. Hence, the data suggested that the mostly raised pectin deposition should be a major factor for Cd accumulation. Meanwhile, the *Osfc16* mutant showed enhanced pectin and hemicellulose rates than those of the WT, in particular for the stem tissue, which should be accountable for much more increased Cd accumulation in the mutant as described above. As uronic acids are the typical components of pectin, this study further observed that the Cd treatments led to much more raised uronic acids levels in the *Osfc16* mutant than the ones in the WT at $p < 0.01$ levels (n

**Table 1**
Lignocellulose composition of rice *Osfc16* mutant and WT incubated with Cd.

| Sample | Tissue | Treatment | Cell wall composition (% DM) | | | | | | |
|---|---|---|---|---|---|---|---|---|---|
| | | | Cellulose | | Hemicellulose | | Lignin | Pectin | |
| WT | Seedling | Control | 17.41 ± 0.17 | | 25.16 ± 0.38 | | 24.80 ± 0.06 | 2.42 ± 0.04 | |
| | | Cd | 13.58 ± 0.29** | −21.99% | 25.75 ± 0.21* | +2.34% | 24.28 ± 0.14 | 2.84 ± 0.03** | +17.11% |
| *Osfc16* | | Control | 16.02 ± 0.48 | | 24.23 ± 0.06 | | 25.30 ± 0.69 | 2.45 ± 0.03 | |
| | | Cd | 10.77 ± 0.35** | −32.73% | 25.23 ± 0.16* | +4.09% | 25.52 ± 0.54 | 3.01 ± 0.02** | +23.00% |
| WT | Stem | Control | 33.99 ± 0.43 | | 18.48 ± 0.44 | | 12.54 ± 0.42 | 3.06 ± 0.03 | |
| | | Cd | 30.90 ± 0.80* | −9.09% | 20.17 ± 0.21* | +9.15% | 12.88 ± 0.19 | 3.82 ± 0.05** | +22.84% |
| *Osfc16* | | Control | 25.56 ± 0.77 | | 22.58 ± 0.15 | | 14.45 ± 0.52 | 3.33 ± 0.13 | |
| | | Cd | 22.96 ± 0.50* | −10.16% | 25.21 ± 0.65* | +11.61% | 14.83 ± 0.50 | 4.74 ± 0.07** | +42.64% |
| WT | Leaf | Control | 29.59 ± 0.59 | | 19.14 ± 0.20 | | 15.80 ± 0.44 | 2.51 ± 0.10 | |
| | | Cd | 27.14 ± 0.39* | −8.27% | 20.25 ± 0.33* | +5.79% | 15.60 ± 0.05 | 3.05 ± 0.02** | +21.71% |
| *Osfc16* | | Control | 23.94 ± 1.49 | | 23.78 ± 0.18 | | 16.45 ± 0.30 | 2.57 ± 0.10 | |
| | | Cd | 20.13 ± 0.58* | −15.93% | 26.07 ± 0.53* | +9.64% | 16.34 ± 0.40 | 3.14 ± 0.03** | +22.08% |

DM as dry matter of biomass. * and ** indicated significant difference between two samples by *t*-test at $p < 0.05$ and 0.01 (n = 3). Increased percentage calculated by subtraction between two samples divided by the control (without Cd incubation). Bar as mean ± SD (n = 3).

= 3) in all tissues examined (Fig. 2A–B); this was confirmed by immunofluorescence detection using specific antibody (CCRC-M38) against uronic acids of pectin (Fig. 2C). By comparison, the *Osfc16* mutant and WT showed large variations of hexoses and pentoses among the three rice tissues from the Cd treatments (Fig. S3). Therefore, the Cd treatment mainly enhanced the uronic acids deposition in the *Osfc16* mutant.

Furthermore, this study detected Cd accumulation with the pectin fractions of young rice seedlings and mature straws (Fig. 2D & E). Despite pectin levels being less than 5% of total lignocellulose residues examined in rice samples (Table 1), this study estimated remarkably high proportions of Cd in the pectin fractions of rice tissues, which accounted for 30%–62% of total Cd detected in rice samples. Notably, the *Osfc16* mutant demonstrated much higher Cd levels than those of the WT in the pectin fractions (Fig. 2F & G), consistent with its much more enhanced Cd accumulation in three tissues described above (Fig. 1). Since uronic acids of pectin could interlink with trace metals *via* chemical bonds (Cheng et al., 2019; Jia et al., 2019; Kartel, Kupchik, & Veisov, 1999), this result suggested that the deposition of uronic acids could be a key factor for much enhanced Cd accumulation in lignocellulose-rich tissues of the *Osfc16* mutant.

### 3.3. Improved biomass saccharification for bioethanol production and Cd collection

As the *Osfc16* mutant has been characterized with high biomass (Li et al., 2017), this study examined if the Cd treatment could further enhance biomass enzymatic saccharification for bioethanol production (Fig. 3). By means of our previously-established approaches, we found that the Cd-treated mutant and WT samples showed significantly higher yields of hexoses (% cellulose) released from enzymatic hydrolyses after mild alkali (0.5%, 1% NaOH) pretreatments were of mature straws (stem, leaf), compared to their control (without Cd) samples (Fig. 3A–C). Further performing yeast fermentation with total hexoses, only partially Cd-treated straw samples showed significantly raised bioethanol yields than those of their controls (Fig. 3D–F), probably due to the released Cd that inhibited yeast fermentation. To understand why the biomass saccharification was significantly enhanced in the Cd-treated samples, this study also detected major lignocellulose recalcitrant factors such as cellulose crystalline index (CrI) and degree of polymerization (DP), and arabinose substitution (xylose/arabinose ratio) of xylans (Fig. 4) (López-Maldonado & Oropeza-Guzmán, 2021). As a result, all Cd-treated straws demonstrated improved lignocellulose recalcitrance relative to their control samples, and particularly, the *Osfc16* mutant had the lowest values of those three recalcitrant factors, consistent with its highest biomass enzymatic saccharification. In addition, because uronic acids of pectin could positively affect biomass enzymatic hydrolyses in bioenergy crops (Wang et al., 2015; Wang et al., 2016), the raised uronic acids from the Cd treatment should be another factor for enhanced biomass saccharification examined in this study.

Assuming that the Cd-treated rice straws could be almost completely digested, this study calculated how much Cd could be released from alkali pretreatments and sequential enzymatic hydrolyses (Table 2). In general, more than 85% of total Cd could be collected from supernatants of pretreatments and enzymatic hydrolyses in both *Osfc16* mutant and WT. In particular, only *Osfc16* mutant released 90% of total Cd after 1% NaOH pretreatment and enzymatic hydrolyses were performed with its stem tissue. Furthermore, the rest of Cd could be collected from the solid residues of yeast fermentation for all rice straw samples. Thereby, the *Osfc16* mutant could not only showed near-complete biomass enzymatic saccharification for bioethanol production as a desirable bioenergy crop, but it also should be considered as the most effective phytoremediation plant for Cd accumulation with lignocellulose tissues *in vivo* and sequential Cd release for collection *in vitro*.

### 3.4. Chemical crosslinking between citrus peels pectin and rice fermentation residues for Cd adsorption

To avoid any biomass residues release into environment during bioethanol conversion, the remaining lignin-rich residues from yeast fermentation were evaluated as biosorbents for trace metal removal, but the adsorption capacity was relatively low (Xu et al., 2020; Xu et al., 2021). As the minor pectin of plant cell walls is predominately

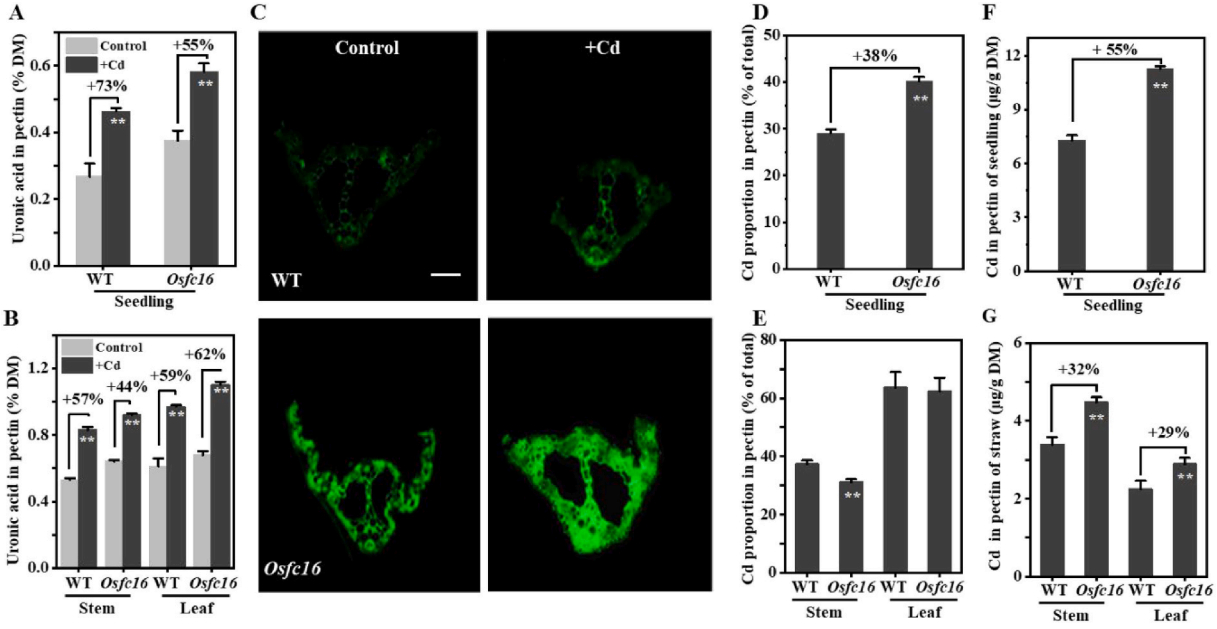


**Fig. 2.** Enhanced pectin deposition with lignocellulose tissues of rice mutant (*Osfc16*) and WT supplied with $CdCl_2$. (A, B) Uronic acids contents of pectin in lignocellulose tissues; (C) *In situ* immunofluorescence observation of pectin epitopes in transverse sections of leaf vein of rice seedlings by using antibody (CCRC-M38) labeled with FITC (green) (scale bar = 100 μm); (D, E) Cd proportion in the pectin fractions of rice samples; (F, G) Cd level in the pectin fractions of rice. "+Cd" as rice seedling supplied with 0.6 mM (141.2 mg/kg water) $CdCl_2$, mature straw tissue (stem, leaf) grown in the soil pots supplied with 100 mg/kg. * and ** indicated significant difference between two samples by *t*-test at $p < 0.05$ and 0.01. Increased percentage calculated by subtraction between two samples divided by the control. Bar as mean ± SD (n = 3).

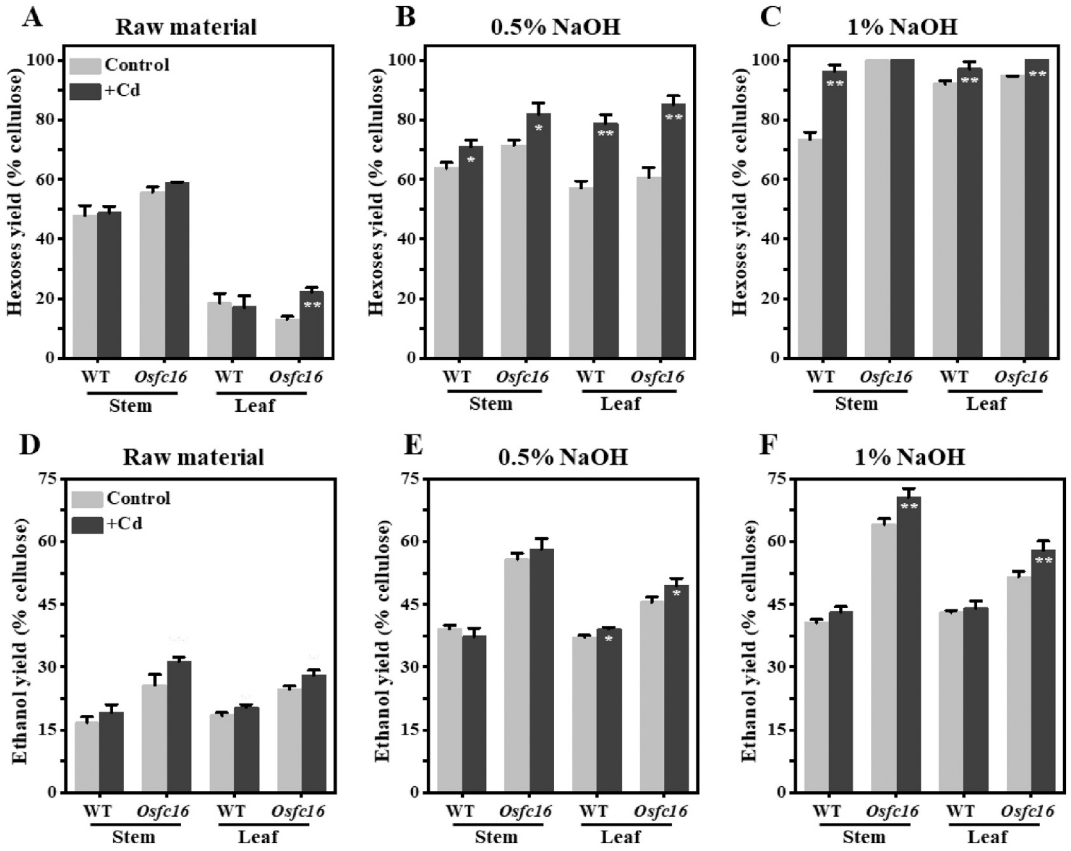


**Fig. 3.** Hexoses and bioethanol yields obtained in rice mutant (*Osfc16*) and WT grown with soil pots supplied with $CdCl_2$. (A, B, C) Hexoses yield released from enzymatic hydrolysis after NaOH pretreatment with mature straw. (D, E, F) Bioethanol yields (% cellulose) by yeast fermentation with the hexoses released from pretreatment and enzymatic hydrolysis as described (A, B, C). * and ** indicated significant difference between two samples by *t*-test at $p < 0.05$ and 0.01 (n = 3). Increased percentage calculated by subtraction between two samples divided by the control. Bar as mean ± SD (n = 3).

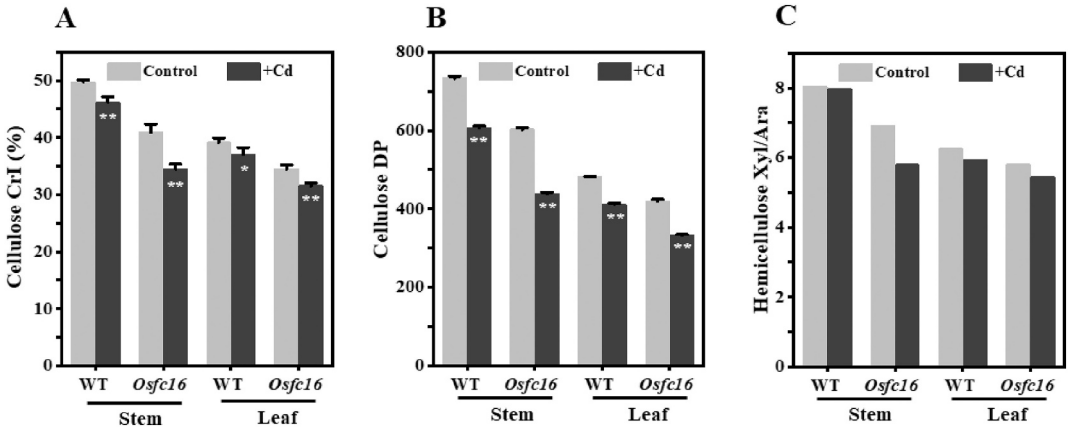


**Fig. 4.** Alteration of cellulose and hemicellulose features in rice mutant (*Osfc16*) and WT grown with soil pots supplied with 100 mg/kg $CdCl_2$ (+Cd). (A) Cellulose CrI; (B) Cellulose DP; (C) Hemicellulose Xyl/Ara. * and ** indicated significant difference between two samples by *t*-test at $p < 0.05$ and 0.01 (n = 3). Increased percentage calculated by subtraction between two samples divided by the control. Bar as mean ± SD (n = 3).

responsible for enhanced Cd adsorption as described above, this study attempted to extract large amount of pectin from citrus peels under different solid-liquid ratios and pH values (Fig. S4), and then perform a chemical crosslinking reaction between the extracted pectin and all remaining biomass residues from yeast fermentation to generate biosorbents by using different concentrations of $H_2O_2$ under three incubation temperatures (Table S1). Integrating different dosages of the citrus peel pectin with the rice fermentation residues, we observed that the *Osfc16* mutant sample showed consistently higher Cd adsorption capacities than those of the WT (Fig. 5A). To test this finding, we conducted classic Cd adsorption analyses by means of our previously-established approaches (Xu et al., 2020; Xu et al., 2021). Under a series of initial Cd concentrations, this study examined much higher Cd adsorption capacities in the fermentation residues of both *Osfc16* mutant and WT, compared to their raw straw materials (Fig. 5B &C), consistent with the previous findings (Xu et al., 2020; Xu et al., 2021; Zeng et al., 2019; Zhang et al., 2018). However, the chemical crosslinking of rice fermentation residues with the pectin of citrus peels, termed as FR-CP

**Table 2**
Cd proportion released from NaOH pretreatment and sequential enzymatic hydrolysis of lignocellulose tissues in rice mutant (*Osfc16*) and WT.

| Sample | Tissue | Total Cd (μg/g) | NaOH pretreatment (%) | Cd in residues (μg/g) | Cd in supernatant (μg/g) | Cd released (% of total) |
|---|---|---|---|---|---|---|
| WT | Stem | 9.09 | 0 | 1.32 | 7.77 | 85.5 |
| | | | 0.5 | 1.08 | 8.01 | 88.1 |
| | | | 1 | 1.08 | 8.01 | 88.1 |
| *Osfc16* | | 14.38 | 0 | 1.74 | 12.64 | 87.9 |
| | | | 0.5 | 1.56 | 12.82 | 89.2 |
| | | | 1 | 1.41 | 12.96 | 90.1 |
| WT | Leaf | 3.54 | 0 | 0.45 | 3.09 | 87.3 |
| | | | 0.5 | 0.40 | 3.14 | 88.7 |
| | | | 1 | 0.37 | 3.16 | 89.3 |
| *Osfc16* | | 4.65 | 0 | 0.61 | 4.04 | 86.9 |
| | | | 0.5 | 0.55 | 4.11 | 88.4 |
| | | | 1 | 0.54 | 4.11 | 88.4 |

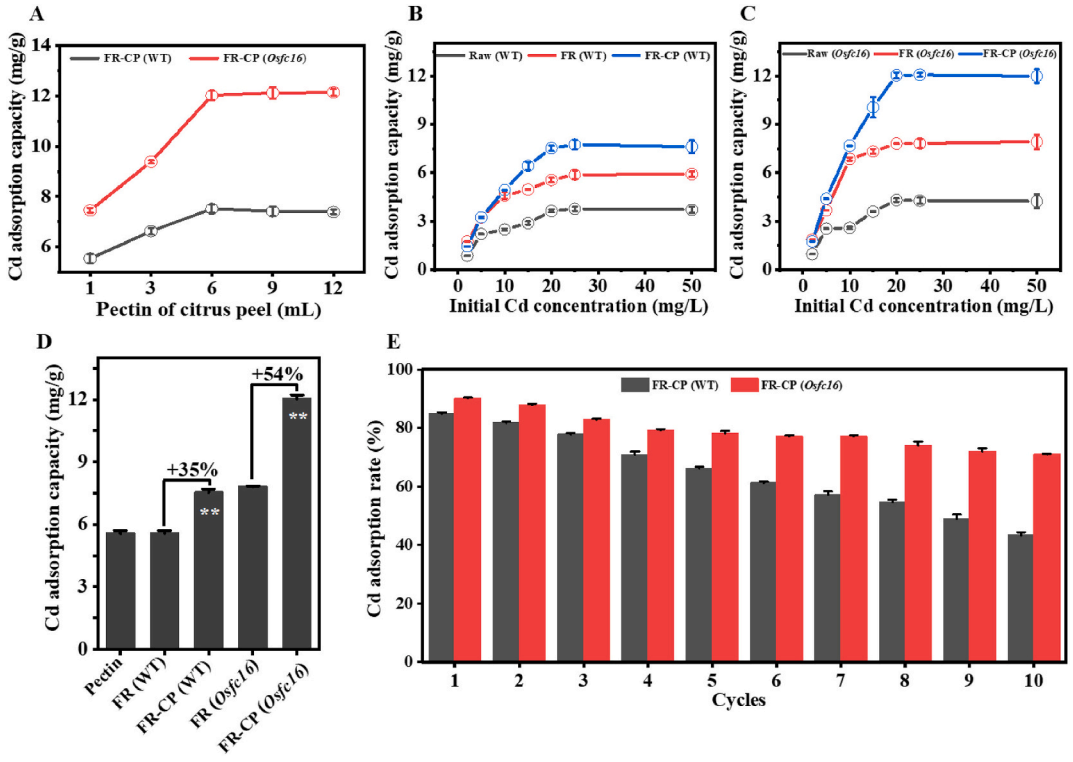


**Fig. 5.** Comparison of Cd adsorption capacity of the fermentation residues (FR) and biosorbents (FR-CP) by chemical crosslinking FR with the pectin extracted from citrus peel. (A) Cd adsorption of the biosorbents crosslinked with different dosage of pectin of citrus peels; (B, C) Cd adsorption under initial Cd concentrations; (D) Cd adsorption capacity of different types of biosorbents; (E) Cycles test of Cd adsorption. FR obtained from enzymatic hydrolysis and yeast fermentation after 1% NaOH pretreatment with mature rice straw. Incubation conditions (A, D), pH = 7.0, $C_0$ = 20 mg/L, biosorbent dose = 1 g/L, $T = 25 \pm 2$ °C, $t$ = 4.0 h, (B) and (C), pH = 7.0, biosorbent dose = 1 g/L, T = 25 ± 2 °C, t = 4.0 h, (E) $C_0$ = 2 mg/L, pH = 7.0, T = 25 ± 2 °C, t = 4.0 h, biosorbent dose = 1 g/L.

biosorbents, showed further raised Cd adsorption capacities than those of the residues by 54% and 35% in the *Osfc16* mutant and WT samples, respectively (Fig. 5D). Consistently, the FR-CP biosorbents had higher Cd adsorptions than those of their fermentation residues under different incubation conditions (temperature, time and pH value) or adding various dosages of biosorbents (Figs. S5 & S6). Furthermore, while the batch experimental data were applied to establish Langmuir and Freundlich isotherm models, the Langmuir model showed extremely high $R^2$ values at more than 0.99, whereas the Freundlich isotherm were of the $R^2$ values ranged from 0.83 to 0.95 (Fig. S7; Table S2), suggesting that the adsorption of Cd on biosorbents better fitted at Langmuir isotherm model. Importantly, the *Osfc16* mutant samples showed higher Cd adsorptions than those of the WT by their FR-CP biosorbents examined in all experimental analyses. In addition, in terms of the 10-time cycling tests of the FR-CP biosorbents, the *Osfc16* mutant sample showed slightly reduced Cd adsorption capacities, whereas the WT sample showed a substantial decrease of Cd adsorption (Fig. 5E). Taken together, therefore, the results indicated that the *Osfc16* mutant could provide the desirable lignin-rich residues to crosslink with the pectin of citrus peels to generate active biosorbents for efficient trace metal adsorption.

### 3.5. Characteristics of biosorbents involved in chemical interaction with Cd

With respects to the chemical-crosslinked biosorbents that were of high Cd adsorption capacity as described above, this study characterized physical and chemical properties of the biosorbents using our previously-established approaches (Xu et al., 2020; Xu et al., 2021). Under scanning electronic microscopy, we first observed a ribbon-like structure of the biosorbents that showed pores of different sizes (Fig. 6A), which could provide large surfaces for chemical crosslinking

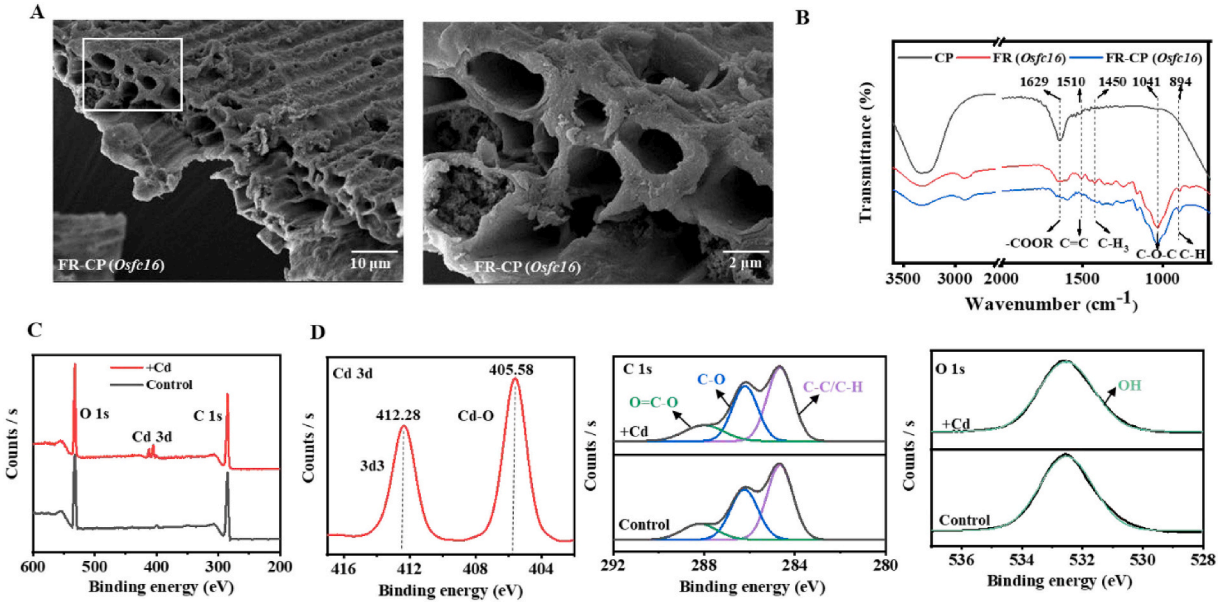


**Fig. 6.** Physical and chemical characterization of biosorbents for Cd adsorption. (A) SEM images; (B) FTIR spectrum; (C) XPS assay; (D) XPS of Cd 3d, C 1s and O 1s spectrum; CP: pectin extracted from citrus peels by ammonium oxalate; FR obtained from enzymatic hydrolysis and yeast fermentation after 1% NaOH pretreatment; FR-CP obtained by $H_2O_2$ oxidation between FR and CP.

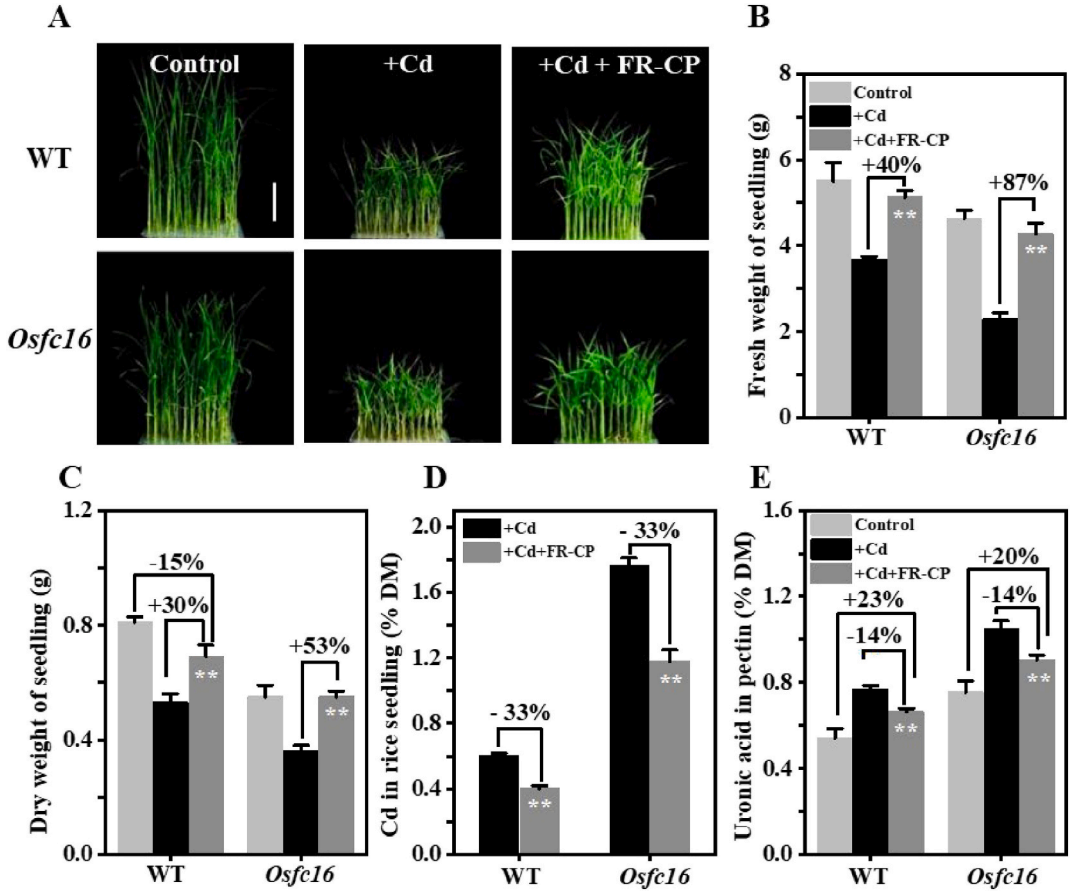


**Fig. 7.** Reduced Cd accumulation with rice seedlings of the *Osfc16* mutant and WT grown in hydroponic culture supplied with pectin-crosslinked biosorbents. (A) Growth of rice seedlings, scale bar = 5 cm; "Control", water only in culture; "+Cd", added with 0.6 mM (141.2 mg/kg water) $CdCl_2$; "+Cd + FR-CP", added with 0.6 mM (141.2 mg/kg water) $CdCl_2$ and the biosorbents at 1 g/L; (B) weight of fresh rice seedlings; (C) dry matter weight of rice seedlings; (D) Cd levels in rice seedlings; (E) uronic acids levels in the pectin fractions. * and ** indicated significant difference between two samples by *t*-test at $p < 0.05$ and 0.01 (n = 3). Increased percentage calculated by subtraction between two samples divided by the sample (+Cd + FR-CP); bar as mean ± SD (n = 3).

between the pectin of citrus peels and the fermentation residues of *Osfc16* mutant. Fourier transform infrared (FTIR) spectroscopy, further showed five altered peaks located at 894 $cm^{-1}$ (C—H), 1041 $cm^{-1}$ (C—O—C), 1450 $cm^{-1}$(–C—$H_3$), 1510 $cm^{-1}$ (C═C) and 1629 $cm^{-1}$ (–COOR) in the biosorbents, compared to either the pectin of citrus peels or the fermentation residues of *Osfc16* mutant straw (Fig. 6B); this confirmed chemical crosslinking between the pectin of citrus peels and the lignin of fermentation residues (Table S3). Meanwhile, XPS was applied to detect metal element interlinkage style, and two typical peaks were observed in the biosorbents incubated with Cd solution, whereas the control (without Cd) did not show those peaks (Fig. 6C). Furthermore, we detected three typical C-linkages of solid residue by XPS, and found that the solid residue incubated with $Cd^{2+}$ exhibited a slight alteration of two peaks (C—C/C—H; C—O), compared to the control without $Cd^{2+}$ (Fig. 6D; Table S4), suggesting that the groups of three peaks should involve in chemical interactions with Cd (Allouche, Mameri, & Guibal, 2011; Taty-Costodes, Fauduet, Porte, & Delacroix, 2003). Therefore, this work demonstrated that the biosorbents were of high Cd adsorption capacity, mainly through typical chemical interaction.

### 3.6. Significantly reduced Cd accumulation by co-supplying pectin-crosslinked biosorbents into hydroponic culture with rice seedlings

To test Cd adsorption capacity in trial of the chemical-crosslinked biosorbents generated from pectin of citrus peels and lignin-rich residues of *Osfc16* biomass fermentation, this study performed hydroponic culture with rice seedlings co-supplied with both high concentration of Cd and low dosage of biosorbents (Fig. 7). While supplied with Cd only, the *Osfc16* mutant and WT obviously showed much defective seedlings phenotypes with relatedly reduced biomass yields (Fig. 7A–C). However, under co-supplements with both Cd and chemical-crosslinked biosorbents, the *Osfc16* mutant and WT were mostly restored from those defective phenotypes with remarkably reduced Cd accumulation in their seedlings (Fig. 7D), consistent with significantly altered uronic acids levels of pectin (Fig. 7E). On the other hand, even though those co-supplements could significantly restore the defective phenotype in the *Osfc16* mutant, it continued to accumulate higher Cd levels than those of the WT in their seedlings; this further confirmed the findings that the *Osfc16* mutant was of relatively enhanced Cd accumulation capacity due to its increased uronic acids deposition. Hence, this study demonstrated that the pectin-crosslinked biosorbents were of remarkably Cd adsorption in rice seedling growth.

### 3.7. Distinct methylene blue adsorption with pectin-crosslinked biosorbents

Although the pectin-crosslinked biosorbents demonstrated high Cd adsorption capacity *in vitro* by chemical interaction as described, this study attempted to test its adsorption capacity with methylene blue (MB), a typical organic dye released from industry factories (Fig. 8). By performing classic adsorption analyses, this study examined that the fermentation residues (FR) of both *Osfc16* mutant and WT were of high MB adsorption capacities under various conditions such as initial MB concentration, incubating temperature, pH and time, and biosorbent dosage. However, the pectin-crosslinked biosorbents (FR-CP) showed obviously higher MB adsorptions than those of the fermentation residues under almost all experiments performed, except the pH values. Notably, either the fermentation residues or the biosorbents from the *Osfc16* mutant sample showed higher MB adsorptions than ones from the WT, consistent with its more raised Cd adsorption as described above.

However, the biosorbents had distinct MB adsorption trends

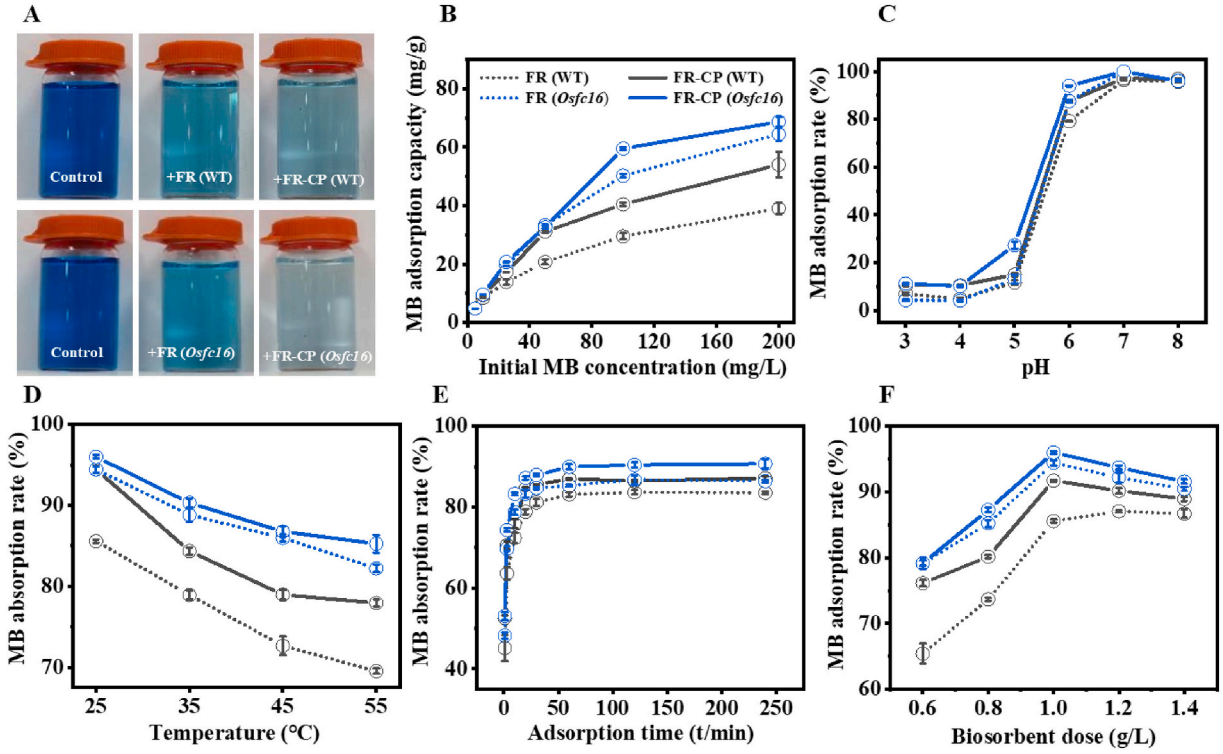


**Fig. 8.** Comparison of the MB adsorption capacities with biosorbents of the *Osfc16* mutant sample under various incubation conditions. (A) Image of MB adsorptions with biosorbens; (B) MB adsorption capacity under different initial MB concentration (C, D, E, F), MB adsorption rates under different pH value, temperature, time and biosorbent dose; FR, Residues obtained from enzymatic hydrolysis and yeast fermentation after 1% NaOH pretreatment; FR-CP, FR crosslinked with the pectin extracted from citrus peels. Incubation conditions: (A), pH = 6.0, biosorbent dose = 1 g/L, T = 25 ± 2 °C, t = 4.0 h. (B), $C_0$ = 10 mg/L, biosorbent dose = 1 g/L, T = 25 ± 2 °C, t = 4.0 h. (C), pH = 6.0, $C_0$ = 10 mg/L, biosorbent dose = 1 g/L, t = 4.0 h; (D), $C_0$ = 10 mg/L, pH = 6.0,T = 25 ± 2 °C, t = 4.0 h; (E), $C_0$ = 10 mg/L, pH = 6.0, biosorbent dose = 1 g/L, T = 25 ± 2 °C.

compared to their adsorption with Cd under different incubation temperatures and pH values. For instances, the MB adsorption reached the maximum at pH 6, whereas the maximum Cd adsorption occurred at pH 9 (Fig. 8C; Fig. S5). Meanwhile, an increase in temperature deceased the absorption of MB but did not alter that of Cd significantly (Fig. 8D; Fig. S5). Further based on the experimental data, both Langmuir and Freundlich model could fit the data for MB as seen from high $R^2$ values (Fig. S8; Table S5), which was different from the Cd adsorption that showed better fit with the Langmuir model described above (Fig. S7; Table S2). As Brunauer–Emmett–Teller (BET) surface area analysis has been well applied to account for biosorbent porosity, this study also determined the surface areas in solid residues, particularly in the residues from the pectin-crosslinked biosorbents (FR-CP), compared to the fermentation residues (FR) of rice straw (Table S6). Particularly, the cross-linked adsorbent showed a 4-fold increase in the specific surface area in the mutant FR-CP, rendering it beneficial for adsorption of Cd and MB. The data also suggested that the pectin-crosslinked biosorbents for adsorption of MB could be relatively complex than that of the Cd adsorption examined in this study.

### 3.8. Synchronous Cd and MB adsorptions with the pectin-crosslinked biosorbents

As the pectin-crosslinked biosorbents (FR-CP) were of high Cd and MB adsorptions, this study further examined its synchronic adsorption capacity *in vitro* by mixing Cd and MB as incubation solution (Fig. 9). In general, both the fermentation residues (FR) and pectin-crosslinked biosorbents showed synchronic adsorption capacity for Cd and MB *in vitro*, but the pectin-crosslinked biosorbents demonstrated relatively higher adsorption levels (Fig. 9A & B). Further compared to the individual Cd or MB adsorption (Fig. S9), the synchronic Cd adsorption rates were much reduced by more than 30% in the WT samples, whereas the synchronic Cd and MB adsorption rates were slightly altered in the *Osfc16* mutant samples (Fig. 9C & D). In particular, the pectin-crosslinked biosorbents of *Osfc16* mutant samples had the same rates of MB adsorption at 94% in both individual and synchronic experiments. Its synchronic Cd adsorption rate was decreased only by 8%, indicating that chemical-crosslinking between the fermentation residues of *Osfc16* mutant and pectin of citrus peels could also generate efficient biosorbents for synchronic removals of trace metal and dye chemical. In addition, as the synchronic adsorption rates of MB were much higher than those of the Cd examined in all samples, it has also explained why the pectin-crosslinked biosorbents could fit both Langmuir and Freundlich isotherm models for maximum MB adsorption, and the only Langmuir model for Cd adsorption. In addition, compared with the previously-reported sorbents generated from biomass residues, the pectin-crosslinked biosorbents showed relatively higher Cd and MB adsorption capacities (Table S7), indicating that the pectin-crosslinked biosorbents should be more affective for both Cd and MB removals.

As one of the most complicated macromolecules in plant cell walls, pectin is of the typical carboxylate and methoxylate groups, and the carboxylate groups act as the chelating cause favor for Cd interaction and MB entrapment (Ibarra-Rodríguez, Lizardi-Mendoza, López-Maldonado, & Oropeza-Guzmán, 2017). As a comparison, the $Cd^{2+}$ could interact with biosorbents *via* a polar covalent bond, whereas the MB should associate with the negative charges of surface functional groups of biosorbent such as carboxyl, carbonyl and hydroxyl (Kumar & Dwivedi, 2019). As the amino and hydroxyl groups of biosorbents could provide a part of adsorption sites, the ion exchange should also occur between the Cd and the trace elements (Na, K, Ca) on the surface of biosorbents (Kumar & Dwivedi, 2019). As chemical interlinking modes of three lignin monomers (H, G, S) mainly include ether bond (β-O-4, 4-O-5, α-O-4) and carbon-carbon bonds (5-5, β-5, β-1, β-β) and the hydroxyl (–OH) and carboxyl groups (–COOH) of lignin can form chemical bonds with pectin (Li, Zhao, et al., 2014; López-Maldonado et al., 2020; Zhang et al., 2021), we assumed that the functional groups of lignin-rich

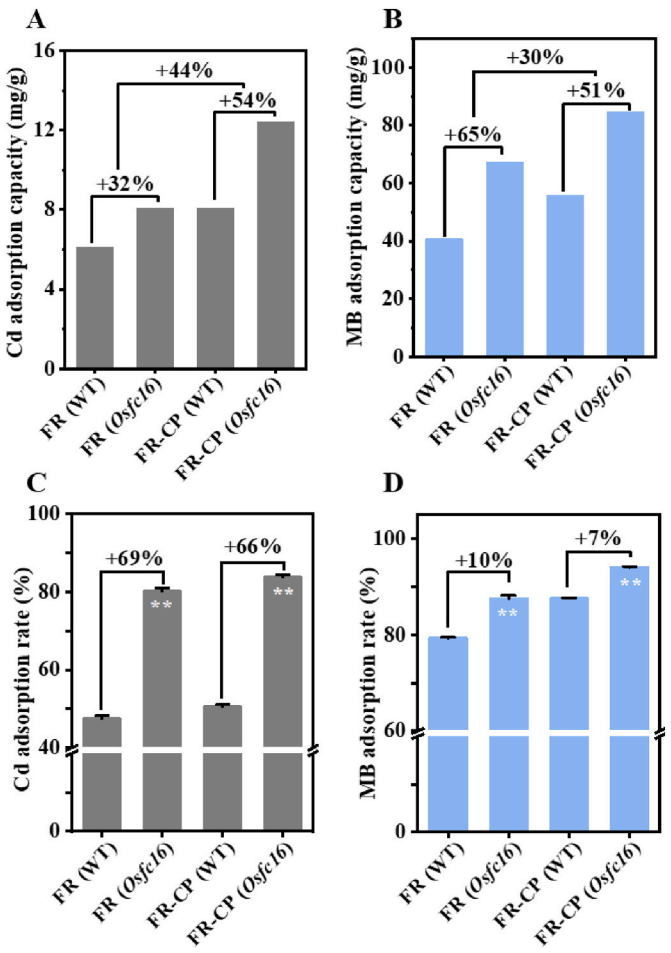


**Fig. 9.** Comparison of synchronous Cd and MB adsorptions. (A, B) Cd and MB adsorption capacity from Langmuir models using biosorbents of rice *Osfc16* mutant and WT samples; (C, D) Synchronous adsorption of biosorbents with Cd and MB; FR: Residues obtained from enzymatic hydrolysis and yeast fermentation after 1% NaOH pretreatment with rice straws in rice *Osfc16* mutant and WT; FR-CP, FR crosslinked with the pectin extracted from citrus peels; Increased percentage calculated by subtraction between two samples divided by the "FR (WT)" or "FR-CP (WT)". Incubation conditions: (C, D), pH = 7.0, biosorbent dose = 1 g/L, $C_{Cd}$ = 2 mg/L, $C_{MB}$ = 10 mg/L, $T = 25 \pm 2$ °C, $t$ = 4.0 h.

biosorbents involved in adsorption with metal ion and dye should be the aliphatic and phenolic hydroxyls (–OH), methoxyls ($–OCH_3$), carbonyls (–C═O), carboxyls (–COOH) and sulfonic ($SO_2$-OH) groups. Due to the electrostatic interaction between the amino group and the hydroxyl group, the Cd and MB molecule may co-share adsorption sites under a competitive action manner. The addition of other metal cations and dyes would compete with the adsorption of Cd and MB, and their adsorption capacity should be reduced due to the limited adsorption sites.

### 3.9. Mechanism of the predominant role of pectin in enhancing in Cd and MB adsorptions and biomass saccharification

Based on all data obtained in this study, we proposed a mechanism model that links all major findings to explain why the *Osfc16* mutant was of consistently enhanced Cd and MB adsorption and biomass saccharification relative to the WT (Fig. 10). Despite that the *Osfc16* mutant has been characterized with significantly reduced lignocellulose recalcitrant factors such as cellulose CrI and DP values and hemicellulose Xyl/Ara ratio, the Cd treatment with the mutant could further improve lignocellulose recalcitrance. These could lead to an integrative enhancement on biomass enzymatic saccharification and bioethanol production

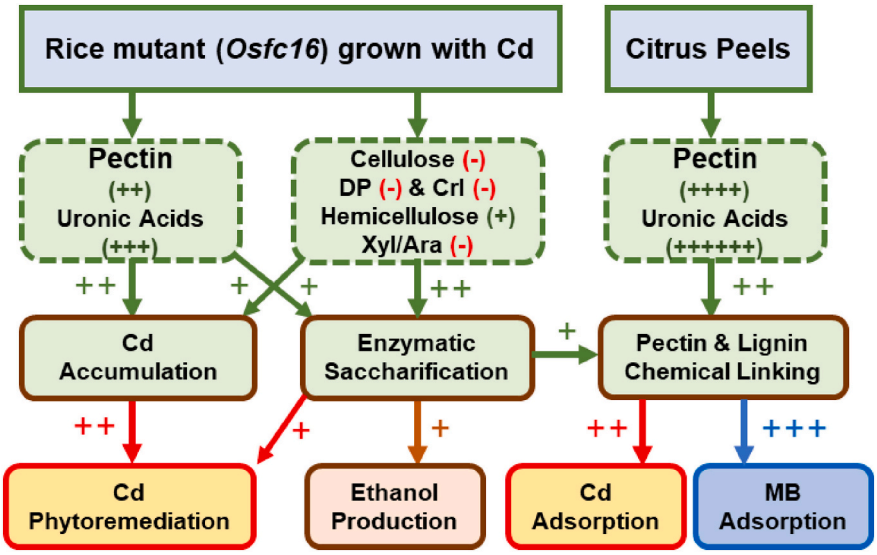


**Fig. 10.** A hypothetic model to elucidate pectin multiple enhancements for Cd and MB adsorptions and biomass saccharification in the *Osfc16* mutant relative to WT. (+) and (−) as positive and negative lignocellulose factors; "+" as enhanced process.

coupled with accumulated Cd to be released. In particular, the *Osfc16* mutant was remarkably rich in uronic acids from pectin, indicating that pectin did play a predominated role for much Cd accumulation with lignocellulose tissues. Meanwhile, the remaining lignin-rich residues after enzymatic hydrolysis and yeast fermentation in the *Osfc16* mutant showed significantly high Cd adsorption capacities than those of the WT, probably due to its near-complete biomass enzymatic hydrolysis for ribbon-like structure with large surfaces and diverse nanopores as described above (Fig. 6A). Furthermore, the fermentation residues of *Osfc16* mutant could be applied to generate active biosorbents for Cd adsorption by chemical crosslinking with the pectin residues extracted from citrus peels. Notably, the biosorbents of *Osfc16* mutant not only showed significantly enhanced Cd adsorption capacity, but also had largely raised MB adsorption. Hence, this model has highlighted the multiple roles of pectin in biomass enzymatic saccharification, trace metal phytoremediation and organic dye removal in the *Osfc16* mutant.

## 4. Conclusion

Using the natural rice mutant (*Osfc16*) defective at cellulose biosynthesis, this study examined enhanced Cd accumulation with lignocellulose tissues than that of the WT, mainly due to significantly raised pectin deposition rich at uronic acids. Meanwhile, the Cd-treatment could further reduce lignocellulose recalcitrance in the *Osfc16* mutant, which enhanced biomass enzymatic saccharification for bioethanol production along with almost all Cd release for recycling. Furthermore, this study used all remaining residues to generate novel biosorbents by chemical crosslinking with the pectin extracted from citrus peels under optimal conditions. Further compared to the WT, the pectin-crosslinked biosorbents showed significantly higher adsorption capacities for Cd and MB, and also showed high synchronic adsorption of MB with Cd, probably due to relatively complicated chemical adsorption process. This study has demonstrated the multiple roles of pectin in Cd and MB adsorptions, and biomass enzymatic saccharification, providing an integrated approach for phytoremediation of trace metal and chemical dye as well as in bioethanol production.

## CRediT authorship contribution statement

**Hua Yu:** Investigation, Methodology, Formal analysis, Writing – original draft. **Meng Hu:** Methodology, Formal analysis, Validation. **Zhen Hu:** Methodology, Formal analysis. **Fei Liu:** Methodology, Formal analysis. **Haizhong Yu:** Methodology, Formal analysis. **Qiaomei Yang:** Validation, Project administration. **Hairong Gao:** Writing – review & editing, Validation. **Chengbao Xu:** Investigation, Methodology. **Meiling Wang:** Formal analysis, Methodology. **Guifen Zhang:** Formal analysis, Methodology. **Yun Wang:** Methodology, Investigation, Resources. **Tao Xia:** Methodology, Investigation. **Liangcai Peng:** Conceptualization, Supervision, Funding acquisition. **Yanting Wang:** Conceptualization, Writing – review & editing, Supervision, Funding acquisition.

## Declaration of competing interest

The authors declare that they have no known competing financial interests or personal relationships that could have appeared to influence the work reported in this paper.

## Acknowledgments

This work was in part supported by the National Science Foundation of China (32101701, 32170268), the Huazhong Agricultural University Independent Scientific & Technological Innovation Foundation (2662020ZKPY013; 2662019PY054), the National 111 Project of Ministry of Education of China (BP0820035), and the Project of Hubei University of Arts & Science (XKQ2018006).

## Appendix A. Supplementary data

Supplementary data to this article can be found online at https://doi.org/10.1016/j.carbpol.2022.119298.

## References

Allouche, F.-N., Mameri, N., & Guibal, E. (2011). Pb(II) biosorption on *Posidonia oceanica* biomass. *Chemical Engineering Journal, 168*(3), 1174–1184.

Baramee, S., Siriatcharanon, A.-K., Ketbot, P., Teeravivattanakit, T., Waeonukul, R., Pason, P., et al. (2020). Biological pretreatment of rice straw with cellulase-free xylanolytic enzyme-producing *Bacillus firmus* K-1: Structural modification and biomass digestibility. *Renewable Energy, 160*, 555–563.

Chen, L., Li, Y., Du, Q., Wang, Z., Xia, Y., Yedinak, E., et al. (2017). High performance agar/graphene oxide composite aerogel for methylene blue removal. *Carbohydrate Polymers, 155*, 345–353.

Chen, Q., Zhao, Y., Xie, Q., Liang, C., & Zong, Z. (2021). Polyethyleneimine grafted starch nanocrystals as a novel biosorbent for efficient removal of methyl blue dye. *Carbohydrate Polymers, 273*, Article 118579.

Cheng, L., Wang, L., Wei, L., Wu, Y., Alam, A., Xu, C., et al. (2019). Combined mild chemical pretreatments for complete cadmium release and cellulosic ethanol co-production distinctive in wheat mutant straw. *Green Chemistry, 21*(13), 3693–3700.
Cheng, S., Yu, H., Hu, M., Wu, Y., Cheng, L., Cai, Q., et al. (2018). *Miscanthus* accessions distinctively accumulate cadmium for largely enhanced biomass enzymatic saccharification by increasing hemicellulose and pectin and reducing cellulose CrI and DP. *Bioresource Technology, 263*, 67–74.
Dmuchowski, W., Gozdowski, D., & Baczewska, A. H. (2011). Comparison of four bioindication methods for assessing the degree of environmental lead and cadmium pollution. *Journal of Hazardous Materials, 197*, 109–118.
Gao, H., Wang, Y., Yang, Q., Peng, H., Li, Y., Zhan, D., et al. (2021). Combined steam explosion and optimized green-liquor pretreatments are effective for complete saccharification to maximize bioethanol production by reducing lignocellulose recalcitrance in one-year-old bamboo. *Renewable Energy, 175*, 1069–1079.
García, O. G. Z., Oropeza-Guzmán, M. T., Argüelles Monal, W. M., & López-Maldonado, E. A. (2019). Design and mechanism of action of multifunctional BPE's with high performance in the separation of hazardous metal ions from polluted water part I: Chitosan-poly(N-vinylcaprolactam) and its derivatives. *Chemical Engineering Journal, 359*, 840–851.
Gurgel, L. V. A., Freitas, R. P. D., & Gil, L. F. (2008). Adsorption of Cu(II), Cd(II), and Pb (II) from aqueous single metal solutions by sugarcane bagasse and mercerized sugarcane bagasse chemically modified with succinic anhydride. *Carbohydrate Polymers, 74*(4), 922–929.
Hameed, B. H., & Ahmad, A. A. (2009). Batch adsorption of methylene blue from aqueous solution by garlic peel, an agricultural waste biomass. *Journal of Hazardous Materials, 164*(2–3), 870–875.
He, B., Hao, B., Yu, H., Tu, F., Wei, X., Xiong, K., et al. (2022). Double integrating XYL2 into engineered *Saccharomyces cerevisiae* strains for consistently enhanced bioethanol production by effective xylose and hexose co-consumption of steam-exploded lignocellulose in bioenergy crops. *Renewable Energy, 186*, 341–349.
Halysh, V., Sevastyanova, O., Pikus, S., Dobele, G., Pasalskiy, B., & Gun'ko, V. M. (2020). Sugarcane bagasse and straw as low-cost lignocellulosic sorbents for the removal of dyes and metal ions from water. *Cellulose, 27*(14), 8181–8197.
Hossain, A., Bhattacharyya, S. R., & Aditya, G. (2014). Biosorption of cadmium by waste shell dust of fresh water mussel lamellidens marginalis: Implications for metal bioremediation. *ACS Sustainable Chemistry & Engineering, 3*(1), 1–8.
Huang, J., Li, Y., Wang, Y., Chen, Y., Liu, M., Wang, Y., et al. (2017). A precise and consistent assay for major wall polymer features that distinctively determine biomass saccharification in transgenic rice by near-infrared spectroscopy. *Biotechnology for Biofuels, 10*(1).
Ibarra-Rodríguez, D., Lizardi-Mendoza, J., López-Maldonado, E. A., & Oropeza-Guzmán, M. T. (2017). Capacity of 'nopal' pectin as a dual coagulant-flocculant agent for heavy metals removal. *Chemical Engineering Journal, 323*, 19–28.
Jensen, M. M., Djajadi, D. T., Torri, C., Rasmussen, H. B., Madsen, R. B., Venturini, E., et al. (2018). Hydrothermal liquefaction of enzymatic hydrolysis lignin: Biomass pretreatment severity affects lignin valorization. *ACS Sustainable Chemistry & Engineering, 6*(5), 5940–5949.
Jia, H., Wang, X., Wei, T., Zhou, R., Muhammad, H., Hua, L., et al. (2019). Accumulation and fixation of cd by tomato cell wall pectin under cd stress. *Environmental and Experimental Botany, 167*, Article 103829.
Jiang, L., Wen, Y., Zhu, Z., Liu, X., & Shao, W. (2021). A double cross-linked strategy to construct graphene aerogels with highly efficient methylene blue adsorption performance. *Chemosphere, 265*, Article 129169.
Jin, W., Chen, L., Hu, M., Sun, D., Li, A., Li, Y., et al. (2016). Tween-80 is effective for enhancing steam-exploded biomass enzymatic saccharification and ethanol production by specifically lessening cellulase absorption with lignin in common reed. *Applied Energy, 175*, 82–90.
Kartel, M. T., Kupchik, L. A., & Veisov, B. K. (1999). Evaluation of pectin binding of heavy metal ions in aqueous solutions. *Chemosphere, 38*(11), 2591–2596.
Kumar, V., & Dwivedi, S. K. (2019). Hexavalent chromium reduction ability and bioremediation potential of *Aspergillus flavus* CR500 isolated from electroplating wastewater. *Chemosphere, 237*, Article 124567.
Li, F., Xie, G., Huang, J., Zhang, R., Li, Y., Zhang, M., et al. (2017). OsCESA9 conserved-site mutation leads to largely enhanced plant lodging resistance and biomass enzymatic saccharification by reducing cellulose DP and crystallinity in rice. *Plant Biotechnology Journal, 15*(9), 1093–1104.
Li, F., Zhang, M., Guo, K., Hu, Z., Zhang, R., Feng, Y., et al. (2014). High-level hemicellulosic arabinose predominately affects lignocellulose crystallinity for genetically enhancing both plant lodging resistance and biomass enzymatic digestibility in rice mutants. *Plant Biotechnology Journal, 13*(4), 514–525.
Li, Y., Liu, P., Huang, J., Zhang, R., Hu, Z., Feng, S., et al. (2018). Mild chemical pretreatments are sufficient for bioethanol production in transgenic rice straws overproducing glucosidase. *Green Chemistry, 20*(9), 2047–2056.
Li, Z., Zhao, C., Zha, Y., Wan, C., Si, S., Liu, F., et al. (2014). The minor wall-networks between monolignols and interlinked-phenolics predominantly affect biomass enzymatic digestibility in *Miscanthus*. *PLoS One, 9*(8), e105115.
Liang, R.-H., Li, Y., Huang, L., Wang, X.-D., Hu, X.-X., Liu, C.-M., et al. (2020). $Pb^{2+}$ adsorption by ethylenediamine-modified pectins and their adsorption mechanisms. *Carbohydrate Polymers, 234*, Article 115911.
Liu, P., Li, A., Wang, Y., Cai, Q., Yu, H., Li, Y., et al. (2021). Distinct *Miscanthus* lignocellulose improves fungus secreting cellulases and xylanases for consistently enhanced biomass saccharification of diverse bioenergy crops. *Renewable Energy, 174*, 799–809.
López-Maldonado, E. A., Oropeza-Guzman, M. T., Jurado-Baizaval, J. L., & Ochoa-Terán, A. (2014). Coagulation–flocculation mechanisms in wastewater treatment plants through zeta potential measurements. *Journal of Hazardous Materials, 279*, 1–10.
López-Maldonado, E. A., Hernández-García, H., Zamudio-Aguilar, M. A. M., Oropeza-Guzmán, M. T., Ochoa-Terán, A., López-Martínez, L. M., et al. (2020). Chemical issues of coffee and tule lignins as ecofriendly materials for the effective removal of hazardous metal ions contained in metal finishing wastewater. *Chemical Engineering Journal, 397*, Article 125384.
López-Maldonado, E. A., & Oropeza-Guzmán, M. T. (2021). Nejayote biopolyelectrolytes multifunctionality (glucurono ferulauted arabinoxylans) in the separation of hazardous metal ions from industrial wastewater. *Chemical Engineering Journal, 423*, Article 130210.
Madadi, M., Wang, Y., Zhang, R., Hu, Z., Gao, H., Dan, Z., et al. (2022). Integrating mild chemical pretreatments with endogenous protein supplement for complete biomass saccharification to maximize bioethanol production by enhancing cellulases adsorption in novel bioenergy *Amaranthus*. *Industrial Crops and Products, 177*, Article 114471.
Murray, A., & Örmeci, B. (2018). Competitive effects of humic acid and wastewater on adsorption of methylene blue dye by activated carbon and non-imprinted polymers. *Journal of Environmental Sciences, 66*, 310–317.
Pattathil, S., Avci, U., Miller, J. S., & Hahn, M. G. (2012). Immunological approaches to plant cell wall and biomass characterization: Glycome profiling. *Methods in Molecular Biology, 908*, 61–72.
Peng, L., Hocart, C. H., Redmond, J. W., & Williamson, R. E. (2000). Fractionation of carbohydrates in *Arabidopsis* root cell walls shows that three radial swelling loci are specifically involved in cellulose production. *Planta, 211*(3), 406–414.
Perazzini, H., Perazzini, M. T. B., Freire, F. B., Freire, F. B., & Freire, J. T. (2021). Modeling and cost analysis of drying of citrus residues as biomass in rotary dryer for bioenergy. *Renewable Energy, 175*, 167–178.
Qu, J., Meng, X., Jiang, X., You, H., Wang, P., & Ye, X. (2018). Enhanced removal of Cd (II) from water using sulfur-functionalized rice husk: Characterization, adsorptive performance and mechanism exploration. *Journal of Cleaner Production, 183*, 880–886.
Rafatullah, M., Sulaiman, O., Hashim, R., & Ahmad, A. (2010). Adsorption of methylene blue on low-cost adsorbents: A review. *Journal of Hazardous Materials, 177*(1–3), 70–80.
Ramrakhiani, L., Halder, A., Majumder, A., Mandal, A. K., Majumdar, S., & Ghosh, S. (2017). Industrial waste derived biosorbent for toxic metal remediation: Mechanism studies and spent biosorbent management. *Chemical Engineering Journal, 308*, 1048–1064.
Safardoust-Hojaghan, H., & Salavati-Niasari, M. (2017). Degradation of methylene blue as a pollutant with N-doped graphene quantum dot/titanium dioxide nanocomposite. *Journal of Cleaner Production, 148*, 31–36.
Saman, N., Tan, J.-W., Mohtar, S. S., Kong, H., Lye, J. W. P., Johari, K., et al. (2018). Selective biosorption of aurum(III) from aqueous solution using oil palm trunk (OPT) biosorbents: Equilibrium, kinetic and mechanism analyses. *Biochemical Engineering Journal, 136*, 78–87.
Taty-Costodes, V. C., Fauduet, H., Porte, C., & Delacroix, A. (2003). Removal of Cd(II) and Pb(II) ions, from aqueous solutions, by adsorption onto sawdust of *Pinus* sylvestris. *Journal of Hazardous Materials, 105*(1–3), 121–142.
Toledo, P. V. O., Bernardinelli, O. D., Sabadini, E., & Petri, D. F. S. (2020). The states of water in tryptophan grafted hydroxypropyl methylcellulose hydrogels and their effect on the adsorption of methylene blue and rhodamine B. *Carbohydrate Polymers, 248*, Article 116765.
Wahlström, N., Steinhagen, S., Toth, G., Pavia, H., & Edlund, U. (2020). Ulvan dialdehyde-gelatin hydrogels for removal of heavy metals and methylene blue from aqueous solution. *Carbohydrate Polymers, 249*, Article 116841.
Wang, Y., Fan, C., Hu, H., Li, Y., Sun, D., Wang, Y., et al. (2016). Genetic modification of plant cell walls to enhance biomass yield and biofuel production in bioenergy crops. *Biotechnology Advances, 34*(5), 997–1017.
Wang, Y., Huang, J., Li, Y., Xiong, K., Wang, Y., Li, F., et al. (2015). Ammonium oxalate-extractable uronic acids positively affect biomass enzymatic digestibility by reducing lignocellulose crystallinity in *Miscanthus*. *Bioresource Technology, 196*, 391–398.
Wang, Y., Liu, P., Zhang, G., Yang, Q., Lu, J., Xia, T., et al. (2021). Cascading of engineered bioenergy plants and fungi sustainable for low-cost bioethanol and high-value biomaterials under green-like biomass processing. *Renewable and Sustainable Energy Reviews, 137*, Article 110586.
Wu, L., Zhang, M., Zhang, R., Yu, H., Wang, H., Li, J., et al. (2021). Down-regulation of OsMYB103L distinctively alters beta-1,4-glucan polymerization and cellulose microfibers assembly for enhanced biomass enzymatic saccharification in rice. *Biotechnology for Biofuels, 14*(1), 245.
Wu, Y., Wang, M., Yu, L., Tang, S.-W., Xia, T., Kang, H., et al. (2020). A mechanism for efficient cadmium phytoremediation and high bioethanol production by combined mild chemical pretreatments with desirable rapeseed stalks. *Science of the Total Environment, 708*, Article 135096.
Xie, H., Zhao, Q., Zhou, Z., Wu, Y., Wang, H., & Xu, H. (2015). Efficient removal of Cd(II) and Cu(II) from aqueous solution by magnesium chloride-modified *Lentinula edodes*. *RSC Advances, 5*(42), 33478–33488.
Xu, C., Xia, T., Wang, J., Yu, L., Wu, L., Zhang, Y., et al. (2020). Selectively desirable rapeseed and corn stalks distinctive for low-cost bioethanol production and high-active biosorbents. *Waste and Biomass Valorization, 12*(2), 795–805.
Xu, C., Zhu, J., Yu, H., Yu, H., Yang, Y., Fu, Q., et al. (2021). Recyclable cascading of arsenic phytoremediation and lead removal coupled with high bioethanol production using desirable rice straws. *Biochemical Engineering Journal, 168*, Article 107950.

Xu, N., Zhang, W., Ren, S., Liu, F., Zhao, C., Liao, H., et al. (2012). Hemicelluloses negatively affect lignocellulose crystallinity for high biomass digestibility under NaOH and $H_2SO_4$ pretreatments in *Miscanthus*. *Biotechnology for Biofuels, 5*(1).

Yang, Q., Zhao, W., Liu, J., He, B., Wang, Y., Yang, T., et al. (2020). Quantum dots are conventionally applicable for wide-profiling of wall polymer distribution and destruction in diverse cells of rice. *Talanta, 208*, Article 120452.

Zeng, G., You, H., Wang, K., Jiang, Y., Bao, H., Du, M., et al. (2019). Semi-simultaneous saccharification and fermentation of ethanol production from *Sargassum horneri* and biosorbent production from fermentation residues. *Waste and Biomass Valorization, 11*(9), 4743–4755.

Zhang, D., VanFossen, A. L., Pagano, R. M., Johnson, J. S., Parker, M. H., Pan, S., et al. (2011). Consolidated pretreatment and hydrolysis of plant biomass expressing cell wall degrading enzymes. *Bioenergy Research, 4*(4), 276–286.

Zhang, H., Yue, X., Li, F., Xiao, R., Zhang, Y., & Gu, D. (2018). Preparation of rice straw-derived biochar for efficient cadmium removal by modification of oxygen-containing functional groups. *Science of the Total Environment, 631–632*, 795–802.

Zhang, G., Wang, L., Li, X., Bai, S., Xue, Y., Li, Z., et al. (2021). Distinctively altered lignin biosynthesis by site-modification of *OsCAD2* for enhanced biomass saccharification in rice. *GCB Bioenergy, 13*(2), 305–319.